environmental microbiology

Environmental Microbiology (2016) **18**(12), 4878–4887 doi:10.1111/1462-2920.13409

Expanded insecticide catabolic activity gained by a single nucleotide substitution in a bacterial carbamate hydrolase gene

Başak Öztürk,[1] Maarten Ghequire,[2] Thi Phi Oanh Nguyen,[1,3] René De Mot,[2] Ruddy Wattiez[4] and Dirk Springael[1]*

[1]*Division of Soil and Water Management, KU Leuven, Leuven, Belgium.*

[2]*Centre of Microbial and Plant Genetics, KU Leuven, Leuven, Belgium.*

[3]*Department of Biology, College of Natural Sciences, Cantho University, Vietnam.*

[4]*Department of Proteomics and Microbiology, University of Mons, Mons, Belgium.*

Summary

Carbofuran-mineralizing strain *Novosphingobium* sp. KN65.2 produces the CfdJ enzyme that converts the *N*-methylcarbamate insecticide to carbofuran phenol. Purified CfdJ shows a remarkably low K_M towards carbofuran. Together with the carbaryl hydrolase CehA of *Rhizobium* sp. strain AC100, CfdJ represents a new protein family with several uncharacterized bacterial members outside the proteobacteria. Although both enzymes differ by only four amino acids, CehA does not recognize carbofuran as a substrate whereas CfdJ also hydrolyzes carbaryl. None of the CfdJ amino acids that differ from CehA were shown to be silent regarding carbofuran hydrolytic activity but one particular amino acid substitution, i.e., L152 to F152, proved crucial. CfdJ is more efficient in degrading methylcarbamate pesticides with an aromatic side chain whereas CehA is more efficient in degrading the oxime carbamate nematicide oxamyl. The presence of common flanking sequences suggest that the *cfdJ* gene is located on a remnant of the mobile genetic element Tn*ceh* carrying *cehA*. Our results suggest that these enzymes can be acquired through horizontal gene transfer and can evolve to degrade new carbamate substrates by limited amino acid substitutions. We demonstrate that a carbaryl hydrolase can gain the additional capacity to degrade carbofuran by a single nucleotide transversion.

Received 19 April, 2016; revised 5 June, 2016; accepted 6 June, 2016. *For correspondence: E-mail: dirk.springael@kuleuven.be; Tel. +32 16 32 16 04; Fax +32 16 3 21997. †Experimental design and writing of the manuscript was done by B.O., R.D.M. and D.S. The main body of laboratory experiments was performed by B.O. M.G designed and supervised the native protein purification from KN65.2. T.P.O.N and R.D.M performed the genomic analysis of KN65.2 LC-ESI-MS/MS proteomic/protein analysis was performed by R.W. All authors have read and approved the manuscript.

Introduction

Carbofuran (2,3-dihydro-2,2-dimethyl-7-benzofuranyl methylcarbamate) is a broad-spectrum carbamate insecticide, nematicide and acaricide that was used in agricultural practice throughout the world. Carbofuran is banned in the European Union and Canada since 2008 because of its high toxicity and high potential for leaching to groundwater (IUPAC), but is still used in countries such as Kenya, Vietnam and South Korea. Degradation by micro-organisms is an important route for carbofuran dissipation in treated soils. Carbofuran-degrading bacteria have been isolated from various geographically separated areas of the world from soils that were regularly treated with the pesticide (Chaudhry and Ali, 1988; Desaint *et al.*, 2000; Yan *et al.*, 2007; Nguyen *et al.*, 2014; Shin *et al.*, 2012, 2014). The Mcd enzyme catalyses the hydrolysis of carbofuran in *Achromobacter* sp. strain WM111 and is encoded by the *mcd* gene (Tomasek and Karns, 1989; Desaint *et al.*, 2000). Mcd is a Mn^{2+} dependent metallohydrolase with carboxylesterase and phosphotriesterase activity (Tomasek and Karns, 1989; Naqvi *et al.*, 2009). This enzyme displays a tandem organization of two metallohydrolase domains with the β-lactamase fold (Pfam PF00144) and cleaves carbofuran into 2,2-dimethyl-2,3-dihydro-1-benzofuran-7-ol (carbofuran phenol) and methylcarbamic acid, which then dissociates into methylamine and CO_2 (Karns and Tomasek, 1991). Mcd homologues have been identified in various other carbofuran-degrading bacteria belonging to various genera including *Achromobacter*, *Rhodococcus* and *Pseudomonas* (Topp *et al.*, 1993; Parekh *et al.*, 1996; Desaint *et al.*, 2000). However, not all carbofuran-degrading isolates carry *mcd* (Shin

et al., 2012). Moreover, *mcd* was never associated with bacteria that mineralize carbofuran completely including the aromatic moiety and growth of Mcd-producing bacteria on carbofuran is rather due to the utilization of the methylcarbamyl side chain as a carbon source (Karns *et al.*, 1986; Topp *et al.*, 1993). This indicates that, in addition to *mcd*, other gene functions are responsible for the first step of carbofuran degradation in microbiota and in particular in carbofuran-degrading bacteria that mineralize the aromatic moiety of carbofuran.

Novosphingobium sp. strain KN65.2 was isolated from carbofuran-exposed agricultural soil in Mekong Delta, Vietnam (Nguyen *et al.*, 2014). This strain, like other reported carbofuran-degrading sphingomonads (Kim *et al.*, 2004; Yan *et al.*, 2007), utilizes carbofuran as sole carbon source with carbofuran phenol as a major intermediate. Mineralization experiments with ^{14}C-aromatic-ring-labeled carbofuran demonstrated the ability of *Novosphingobium* sp. KN65.2 to degrade the aromatic ring of carbofuran and use it a carbon source (Nguyen *et al.*, 2014). Strain KN65.2 metabolizes carbofuran via a unique operon consisting of the *cfd* genes. The oxygenase genes *cfdC* and *cfdE* were suggested to be involved in the processing of carbofuran phenol and *cfdG* and *cfdH* are likely to be involved in the conversion of coenzyme A-activated intermediates (Nguyen *et al.*, 2014). The enzyme which converts carbofuran to carbofuran phenol, however, could not yet be identified. The KN65.2 genome lacks the *mcd* gene but carries the gene *cfdJ*, a close homologue of the carbaryl hydrolase gene *cehA* (Nguyen *et al.*, 2015) of *Rhizobium* sp. strain AC100 that converts the carbamate compound carbaryl (1-naphthyl methylcarbamate) to 1-naphthol and methylamine (Hashimoto *et al.*, 2002). Interestingly, CehA also hydrolyses several other carbamate pesticides but has no catabolic activity towards carbofuran (Hashimoto *et al.*, 2002). In this paper, we demonstrate the ability of CfdJ to hydrolyse carbofuran and investigate how the few amino acid differences between CfdJ and CehA influence carbamate substrate specificity.

Results

Identification of the carbofuran hydrolase CfdJ in Novosphingobium *sp. KN65.2*

Protein fractions showing conversion of carbofuran into carbofuran phenol were obtained after anion exchange, cation exchange and hydrophobic interaction chromatography (HIC) of *Novosphingobium sp.* KN65.2 cell extracts. Peptide sequences generated from these fractions by MS/MS analysis were compared to public databases (NCBI nr database) and the annotated KN65.2 draft genome sequence. As shown in Supporting Information Table T1, more than 80% of the sequences matched to the carbaryl hydrolase CehA from *Rhizobium* sp. AC100 (Hashimoto *et al.*, 2002) suggesting that the corresponding protein in strain KN65.2 is responsible for the observed carbofuran hydrolysis activity in the protein extract. This putative carbofuran hydrolase was named as CfdJ and the corresponding gene as *cfdJ* in analogy with the Cfd enzymes/*cfd* genes specifying the degradation of carbofuran phenol in strain KN65.2. Both CehA and CfdJ have the same size (794 amino acids), including a 29-amino acid N-terminal signal peptide that is lacking in mature CehA purified from AC100 cells (Hashimoto *et al.*, 2002). This indicates that CehA is translocated to the periplasm via the Sec or TAT system and that CfdJ is likely directed to the same subcellular location. Remarkably, these two proteins differed from each other at only four amino acid residues, F or L (152), G or A (207), T or A (494), and I or T (570) in CehA or CfdJ, respectively. At the DNA level this is due to single G↔C transversions (amino acids 152 and 207) and single transitions (A↔G, amino acid 494; T↔C, amino acid 570). There is one additional but silent T↔C transition (F498). The rest of the coding sequences of *cehA* and *cfdJ* are identical.

The *cehA* gene is located on a mobile genetic element (Tn*ceh*) bordered by two IS elements (IS*Rsp3*) of the IS*21* family (Hashimoto *et al.*, 2002). The IS element carries a transposase gene pair (*istA*-*istB*) that is flanked by terminal inverted repeats (IR, 30 bp). The *cfdJ*-containing contig (3456 bp) in the draft genome of strain KN65.2 carries the same IR and a truncated *istB* gene (with a potential new start codon) upstream of *cfdJ*. The *cfdJ* downstream region is also conserved and encodes a short ORF encoding a hypothetical protein (151 amino acids; not annotated on Tn*ceh*). No additional Tn*ceh* sequences can be retrieved in the KN65.2 genome, suggesting that only part of the mobile element is retained in *Novosphingobium*. The same IS element is also present in the choloroanilide-degrading *Sphingomonas* sp. DC-6 where it is linked to the oxygenase component CndA of the three-component Rieske non-heme iron oxygenase catalyzing the *N*-dealkylation of chloroacetanilide herbicides (Chen *et al.*, 2014) (Fig. 1).

CfdJ is active on naphthyl- and phenyl-substituted methylcarbamates

The N-terminal His-tagged CfdJ protein was purified by affinity chromatography to determine degradation kinetics and the substrate specificity. The size of the purified CfdJ protein closely matched the expected 87.6 kD size on SDS-PAGE (Fig. 2). CfdJ kinetics followed Michaelis-Menten kinetics until a concentration of 0.7 mM. Higher concentrations resulted in decreasing conversion rates (Fig. 3). The Vmax, K_M and the rate constant *kcat* of CfdJ for carbofuran were estimated as 0.39 ± 0.2 μM min^{-1}, 0.53 ± 0.05 μM and 11.46 ± 0.57 s^{-1}, respectively.

To study the substrate specificity of CfdJ, different carbamate compounds were incubated for 2 h with the enzyme.

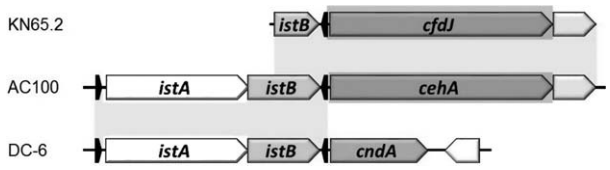

Fig. 1. Schematic representation of the *Novosphingobium* sp. KN65.2 genomic region carrying the *cfdJ* gene and the corresponding fragment of the transposon bearing the *cehA* gene in *Rhizobium* sp. AC100.
The ISRsp3 element with transposase genes *istA* and *istB* is delineated by black arrowheads (inverted repeats). The position of the ISRsp3-linked *cndA* gene of *Sphingomonas* sp. DC-6 is shown for comparison. The grey and white arrows represent ORFs for hypothetical proteins. The near identical DNA sequences are connected by shaded boxes.

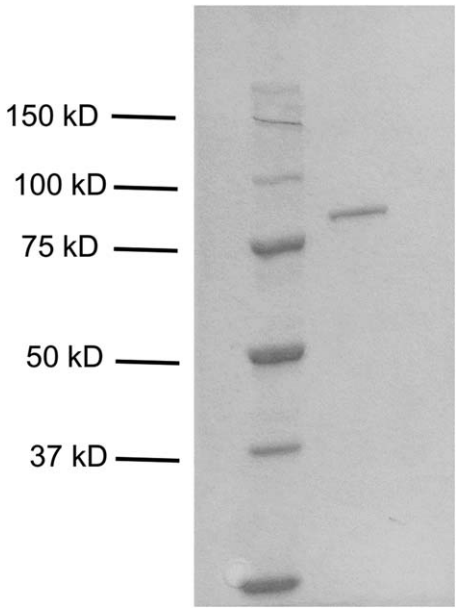

Fig. 2. Purified His-tagged CfdJ protein from *E. coli* carrying pCfdJ_NH.
The size standard is the Precision Plus Protein Unstained Protein Standard (Biorad). The position of CfdJ in the gel agrees with the expected size of the purified protein, i.e., 87,6 kDa

The extent of hydrolysis of carbofuran was about 0.6-fold compared to carbaryl. CfdJ degraded all tested methylcarbamate pesticides with a phenyl side chain well. Conversely, the oxime methylcarbamates oxamyl and aldicarb appeared to be relatively poor substrates (Fig. 4). CfdJ also degraded 4-nitrophenyl acetate indicative of esterase activity (data not shown).

CfdJ and CehA: founding members of a new protein family

The homology search with the CfdJ amino acid sequence returned 17 unique proteins. In addition to *cehA* from *Rhizobium* sp. AC100, close homologues (99% identity on amino acid level) of CfdJ are also present in a number of pseudomonads utilizing oxamyl as sole carbon source (Rousidou *et al.*, 2016). The nucleotide sequences of the *cfdJ* homologues in those oxamyl degrading strains are either identical to this of *cehA* (in *Pseudomonas monteilii* OXA18) or differ from *cehA* at two nt positions (in *Pseudomonas extremaustralis* OXA17, *Pseudomonas jinjuensis* OXA20, and *P. monteilii* OXA25), i.e., a C-to-A transversion (resulting into a T-to-N substitution at amino acid position 477) in addition to the silent T↔C transition (F498) also present in *cfdJ*.

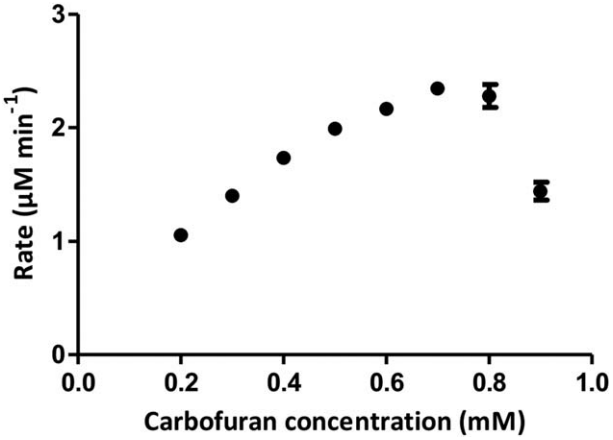

Fig. 3. Degradation of carbofuran by CfdJ plotted against the substrate concentration.
The enzyme activity is expressed in terms of µM carbofuran phenol produced per minute. Error bars indicate standard deviation (n = 3).

The other 15 proteins were all hypothetical proteins with less than 50% identity to CfdJ. They originated from bacteria with diverse phylogenetic background including members of the *Planctomycetes-Verrucomicrobia-Chlamydiae* superphylum, *Bacteroidetes*, *Acidobacteria*, and *Actinobacteria*, but no other Proteobacteria (Fig. 5). All sequences contain a Sec or TAT signal peptide. The amino acid differences between CehA and CfdJ proteins, with the exception of the F to L substitution in position 152, are within the conserved region (Supporting Information Fig. F1).

An amino acid substitution between CehA and CfdJ is decisive for carbofuran hydrolysis

Despite the fact that only a few amino acids differ between CehA and CfdJ, CehA does not transform carbofuran (Hashimoto *et al.*, 2002). Carbaryl hydrolytic activity and lack of activity on carbofuran of CehA was confirmed using recombinant CehA. To determine which amino acid substitution(s) determine the shift of substrate specificity from carbaryl only to both carbofuran and carbaryl, a series of recombinant CfdJ/CehA hybrids were tested for the conversion of carbaryl and carbofuran in comparison with CehA and CfdJ. The hybrid proteins were constructed as

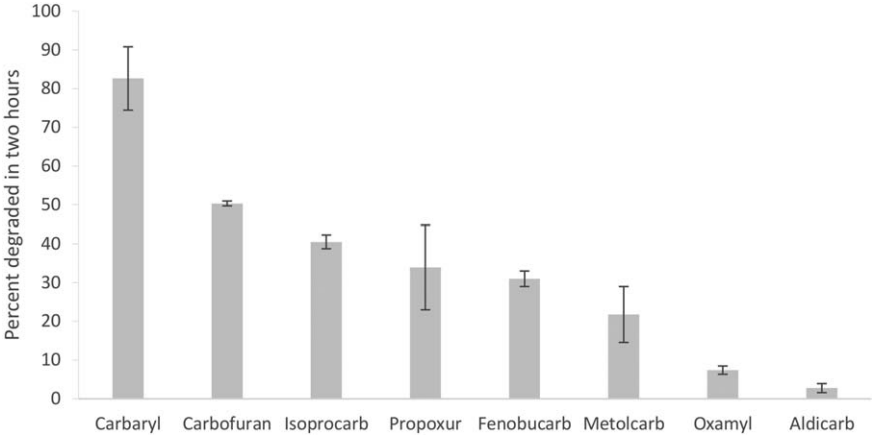

Fig. 4. Substrate specificity of CfdJ towards different carbamate compounds. The percentage of the initial carbamate concentration (0.5 mM) degraded by CfdJ was determined after two-hour incubation. Values are averages of triplicates and the error bars indicate the standard deviation.

such that in each hybrid one of the four amino acids that differed between CfdJ and CehA was substituted in CfdJ with the corresponding one in CehA (Fig. 6A). The hybrid recombinant proteins were named, LAAI, LATI, LGTI, and FAAT, according to the order of the four amino acid substitutions. Like their parent enzymes, all hybrids readily transformed carbaryl. The hybrids (LAAI, LATI, LGTI) showed reduced carbofuran hydrolytic activity compared to this of CfdJ, while a single substitution from $L_{(152)}$ to $F_{(152)}$ (hybrid FAAT) rendered CfdJ completely inactive against carbofuran (Fig. 6B–D). Oxamyl was additionally tested as an aliphatic carbamate. LAAI, LATI and LGTI

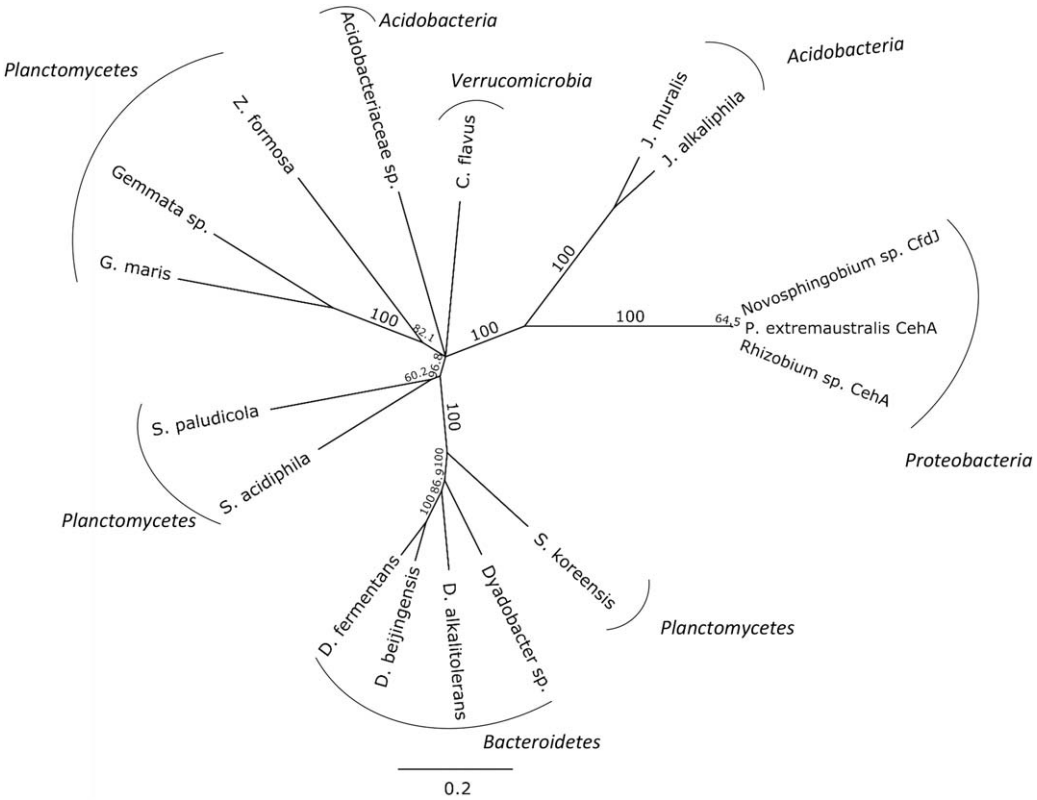

Fig. 5. Phylogenetic analysis of CfdJ and its closest relatives.
Multiple alignment of the amino acid sequences was used to construct a maximum likelihood tree. Both characterized and hypothetical proteins were included in the analysis. The proteins included in the tree, their bacterial hosts and corresponding accession numbers of their aligned amino acid sequences can be found in the Supporting Information Materials section, Supporting Information Table T2. The main phyla to which the bacterial isolates belong are indicated. The scale bar represents 0.2 substitutions per site and bootstrap values (percentages of 1000 repeats) are indicated on the branches.

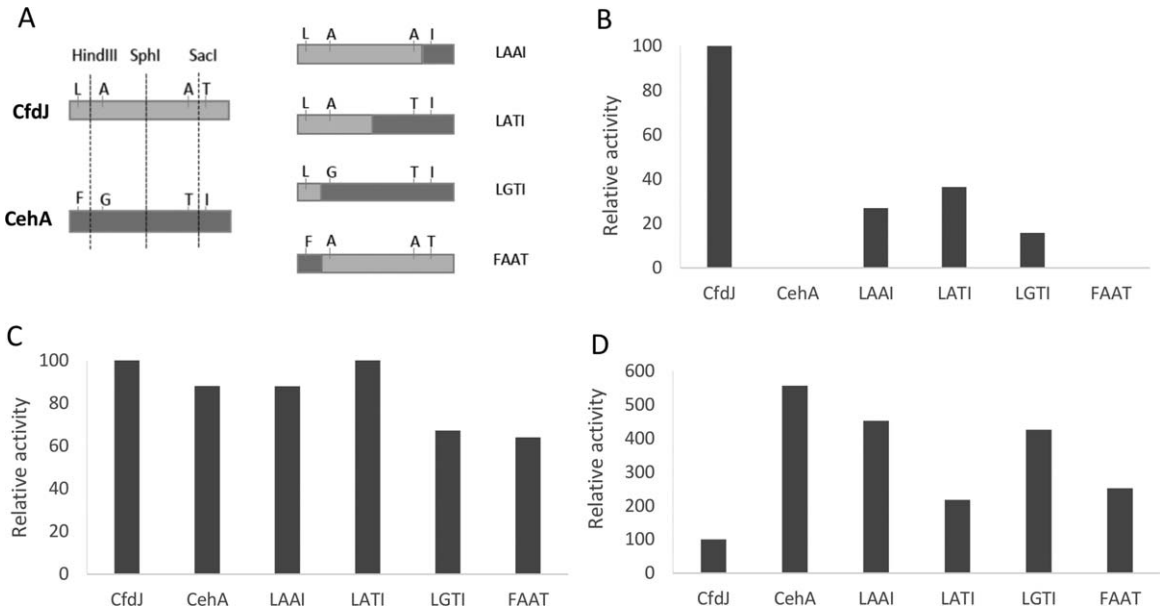

Fig. 6. Construction of CfdJ-CehA hybrids and their degradation activity towards carbamate substrates. (A) Restriction sites and cloning scheme for the construction of the CfdJ-CehA hybrids.
The *cfdJ* and *cehA* amplicons were cut with the appropriate enzyme and the ligated complementary fragments cloned into the plasmid pET28a. (B–D) Degradation activity for carbofuran (B), carbaryl (C) and oxamyl (D) by CehA and CfdJ hybrids relative to the wild-type CfdJ. The activity of CehA and variants are expressed as percentages of the CfdJ activity. The values are the average of two independent experiments, with less than 15% variance.

transformed oxamyl, much better than CfdJ but still not as efficiently as CehA.

Discussion

This study is the first report of the identification of a carbofuran-hydrolyzing enzyme in carbofuran-mineralizing sphingomonads. Sphingomonads play an important role in carbofuran removal in the environment since worldwide most of the bacterial isolates that use carbofuran as sole source of carbon and energy, involving mineralisation of the aromatic ring moiety, are sphingomonads. This is in contrast to other carbofuran-degrading bacteria that convert carbofuran into carbofuran phenol with the Mcd enzyme but without further degrading this catabolite and using released methylamine as carbon source. In this paper, we show that carbofuran degradation in *Novosphingobium* sp. KN65.2 is catalysed by an enzyme that has no similarity to Mcd. Instead, *Novosphingobium* sp. KN65.2 produces CfdJ, an enzyme with nearly identical amino acid sequence to CehA. The latter hydrolase was previously identified in *Rhizobium* sp. AC100 that degrades the structurally related pesticide carbaryl.

The near nucleotide sequence identity of *cehA* and *cfdJ* and available flanking regions suggest that *cfdJ* was originally part of a transposable element. In analogy with other catabolic genes (Springael and Top, 2004), it can be assumed that *cfdJ* was acquired by strain KN65.2 through horizontal gene transfer and hence that horizontal gene transfer events contributed to carbofuran metabolism in strain KN65.2.

The kinetic properties of the CfdJ protein towards carbofuran are significantly different from those of Mcd. The K_M values of Mcd towards carbofuran (63 μM; (Karns and Tomasek, 1991)) and carbaryl [31 μM; (Naqvi *et al.*, 2009)] suggest that its substrate affinity is similar to those for carbaryl of *Rhizobium* CehA [62 μM; (Hashimoto *et al.*, 2002)] and the *Blastobacter* M501 methylcarbamate hydrolase [55 μM; (Hayatsu and Nagata, 1993)] However, these values are about two orders of magnitude larger than that of CfdJ acting on carbofuran. The K_M of CfdJ towards carbofuran is comparable to this of the amidase BbdA for 2,6-dichlorobenzamide, which displays one of the lowest K_M values reported for a xenobiotic-degrading enzyme (T'Syen *et al.*, 2015). This low value indicates the high affinity of CfdJ towards carbofuran, but this can also affect reaction rates due to tight binding of the substrate to the enzyme (Northrop, 1998).

CfdJ and CehA lack any sequence similarity to the metallohydrolase Mcd in which no equivalent secretory signal is present. The same holds for the CahA from *Arthrobacter* sp. RC100, a member of the amidase signature family (Pfam PF01425) that degrades carbaryl but has higher activity on isobutyramide (Hashimoto *et al.*, 2006). These two proteins also do not contain any other previously described conserved domain. The amino acid sequences

of CfdJ and CehA however share conserved regions with a group of hypothetical proteins, and these together constitute a putative novel protein family. The non-proteobacteria producing CehA/CfdJ-related proteins are generally isolates from pristine environments and not typically associated with degradation of pollutants introduced by anthropogenic activities, suggesting that these enzymes may play a role in the degradation of natural products. Secondary metabolites with striking similarity to the phenyl carbamate pesticides (e.g., physostigmine) are produced by certain plants such as calabar bean (*Physostigma venenosum*) and some actinomycetes such as *Streptomyces griseofuscus* (Liu *et al.*, 2014). With the exception of the actinobacterial proteins, all these sequences contain a predicted Sec or TAT signal peptide, indicating that most members of this novel family fulfil extracytoplasmic functions.

Using the amino acid sequence of the *Rhizobium* CehA protein as a reference, the unique substrate specificity of the CfdJ protein towards carbofuran can be linked to four candidate amino acids that are the only residues that differ between CfdJ and CehA. The results with the CfdJ mutants show that a single amino acid change from F to L in residue 152 in CehA results in the gain of carbofuran hydrolysis ability, whereas the opposite substitution in CfdJ leads to the loss of this activity and therefore this amino acid switch between hydrophobic amino acids with an aliphatic side chain and an aromatic moiety appears crucial for substrate specificity. The three other amino acid substitutions between CfdJ and CehA do affect the enzyme's carbofuran hydrolysis capacity, although they do not have the determining effect of the F-to-L substitution at position 152. Crystallization and 3D structure determination will be instrumental to elucidate the molecular basis of the enzyme's substrate recognition. In-depth characterization of the LGTT and LGAT hybrids could provide information about other residues that are important for recovering full carbofuran degradation activity. This knowledge will be important for designing strategies leading to evolved protein variants that are capable of degrading related pesticides.

The sequence around residue 152 represents one of the regions with low sequence conservation among proteins of the CehA/CfdJ family and in most of the hypothetical relatives the equivalent position of CfdJ key residue 152 is occupied by a polar or charged amino acid. Apparently, this part of the protein is subject to mutations that enable adaptation to new substrates, while not affecting correct folding of the protein.

The substrate specificity of CfdJ shows that the enzyme recognizes a broad range of carbamate pesticides as well as the esterase substrate 4-nitrophenyl acetate, which is consistent with the findings for CehA. Although the enzyme degrades carbofuran in contrast to CehA, it still degrades carbaryl more efficiently than carbofuran, indicating that the enzyme possibly evolved from a carbaryl-degrading enzyme. Compared to CehA, CfdJ degrades propoxur, isoprocarb and fenobucarb more efficiently (Hashimoto *et al.*, 2002). In contrast to the carbamate pesticides with a phenolic side chain, the aliphatic carbamate pesticide oxamyl is more efficiently degraded by the CehA and all CfdJ variants than by CfdJ. Apparently, the four amino acid residues in which CfdJ and CehA differ are instrumental in not only differentiating between carbofuran and carbaryl but other carbamate pesticides as well suggesting that slight mutations at these positions can dramatically change substrate specificity including other carbamate pesticides. It has been demonstrated before that minor amino acid substitutions can have determining effects on an enzyme's activity and substrate preference. In the case of melamine deaminase TriA and atrazine chlorohydrolase AtzA, a difference of only nine amino acids exists between these two enzymes but AtzA cannot recognize melamine and TriA cannot recognize atrazine (Seffernick *et al.*, 2001). As for CfdJ, one amino acid change from glutamine in AtzA to aspartate in TriA at residue 125 has a determining effect on the enzyme's activity (dechlorination vs deamination) (Noor *et al.*, 2012). A recent study on the crystal structure of the AtzA has revealed that this amino acid substitution affects the active site geometry (Peat *et al.*, 2015). Between AtzA and TriA, just like in the case of CfdJ and CehA, only a single silent mutation is evident. This indicates that a strong selection pressure leads to the rapid changes in the amino acid composition that enables the organism to adapt to new substrates (Seffernick *et al.*, 2001) as weak selection pressure often yields silent mutations that correct for codon bias (Jukes, 1980; Akashi, 1999). Noor *et al.* (2014) recently showed that evolution of AtzA is ongoing by identifying AtzA homologues in different triazine degrading bacteria in which single amino acid substitutions determined triazine substrate range. The transition of amino acid position residue 152 from F to L between CehA and CfdJ is due to a single nucleotide change showing that minimal genetic change can have a major impact on degradation capacity.

Conclusion

Our findings provide further evidence that catabolic genes are readily transferred between the members of microbial communities through horizontal gene transfer and that the corresponding enzymes can evolve rapidly under selective pressure to adapt for degradation of new substrates. By scrutiny of two enzymes involved in degradation of methylcarbamate insecticides, we revealed that minor nucleotide changes affecting only four residues in the sphingomonad enzyme CfdJ and the rhizobial enzyme CehA suffice to generate different substrate profiles. Most strikingly, for

Table 1. Plasmids and strains used in this study.

Plasmids/strains	Description	Source
Novosphingobium sp. KN65.2	Carbofuran-degrading strain	Nguyen *et al.*, (2014)
E. coli DH5α	F^- endA1 glnV44 thi-1 recA1 relA1 gyrA96 deoR nupG purB20 ϕ80dlacZΔM15 Δ(lacZYA-argF)U169, hsdR17(rK^-mK^+), λ^-	Invitrogen
E. coli BL21 (DE3)	F^- ompT gal dcm lon hsdSB(rB^- mB^-) λ(DE3 [lacI lacUV5-T7 gene 1 ind1 sam7 nin5])	New England Biolabs
pET28a	Expression vector, kanR	Novagen
pUCIDT-Kan	Cloning vector, kanR	Integrated DNA Technologies

these members of a new protein family we demonstrated that a single nucleotide change in a poorly conserved region suffices to expand its carbamate pesticide substrate range.

Experimental procedures

Bacterial strains, plasmids, and culture conditions

Bacterial strains and plasmids used in this study are described in Table 1. *Novosphingobium* sp. strain KN65.2 was routinely grown on Trypticase Soy Broth and agar at 25°C. *Escherichia coli* was cultured in lysogeny broth (LB, 2.5%) at 37°C.

Purification and identification of the KN65.2 carbofuran hydrolase CfdJ

KN65.2 was grown in 2 L of TSB medium to an OD_{600} of 1. Cells were harvested at 4 000 g for 15 min, washed three times with deionized water and the cell pellet was frozen at −20°C overnight. The cells were resuspended in 25 mL Q running buffer (50 mM TrisCl, 20 mM NaCl, pH 7.5) and sonicated at 40% amplitude for 15 min, with 30-second on-off cycles in a VibraCell VCX 13 sonicator (Sonics, Newtown, CT). The lysate was centrifuged at 21 000 g for 30 min and the supernatant was filtered through a 0.22 μM filter. The proteins in the filtrate were separated on a 5 mL Q-column (GE Healthcare Life Sciences, Diegem, Belgium) using an Äkta Purifier fast protein liquid chromatograph (FPLC) (GE Healthcare). Proteins were eluted with a linear NaCl gradient (0.2 to 1 M, 100 mL) in Q buffer. Active fractions were pooled and dialyzed against the SP running solution (50 mM acetic acid, pH 4.8) overnight. The protein solution was passed through a 1 mL HiTrap SP HP column (GE Healthcare) and proteins eluted with a linear NaCl gradient (0 to 1 M, 100 mL) in SP buffer. Active fractions were again pooled and supplemented with ammonium sulfate buffer (1.7 M, 20 mM Tris-HCl, pH 7.5) to a final concentration of 1 M. The sample was loaded on a Phenyl Sepharose HIC HP column (GE Healthcare) and fractions were eluted with a linear gradient of ammonium sulfate (1.0 M to 0 M). To determine carbofuran hydrolase activity in the protein fractions, 10 μL of each fraction was incubated with 990 μL of 1 mM carbofuran in sodium phosphate buffer, pH 7.3. The formation of carbofuran phenol (Dr. Ehrenstorfer GmbH, Augsburg, Germany) was measured using reverse-phase ultrahigh performance liquid chromatography (RP-UHPLC) on a Nexera (Shimadzu Corp, Kyoto, Japan) apparatus equipped with a Platinum EPS C18 column, 150 × 4.6 mm (Grace, Columbia, MD) and a UV–Vis spectrometer and using 30% acetonitrile in water as eluent. The retention times for carbofuran and carbofuran phenol were 4.8 and 4.3 min, respectively. The detection limit for both carbofuran and carbofuran phenol was 10 μM. Active protein fractions obtained after HIC purification were examined for purity on a 10% SDS-PAGE gel, pooled, and analyzed by liquid chromatography-electrospray ionization-tandem mass spectrometry (LC-ESI-MS/MS) as described previously (Breugelmans *et al.*, 2010).

Expression and purification of CfdJ

Genomic DNA from KN65.2 was extracted using a standard cetyltrimethylammonium bromide DNA extraction protocol (Larsen *et al.*, 2007). The *cfdJ* gene was cloned in parallel with and without a His-tag to examine a possible tag effect. To this end, the *cfdJ* gene was amplified from KN65.2 genomic DNA with either forward primer CfdJ_NH_F (5′-CGCGGATCCTCGACTGACGCAATTGAGCC −3′) for cloning the gene with a His-tag or primer CfdJ_or NN_F (5′-CCATGGCCTCGACTGACGCAATTGAGCC-3′) for cloning without a His-tag. The reverse primer was CfdJ_NH_R in both cases (5′- CGCGAATTCTCACGTTAAGTCGCTTTCGGC-3′). The PCR was performed in 50 μL reactions containing 1.25 U of DreamTaq polymerase in 1X PCR buffer (Thermo Fischer Scientic, Leuven, Belgium), 200 μM of each dNTP, 0.1 μM of forward and reverse primer and 100 ng of template DNA. PCR reactions consisted of 5 min initial denaturation at 94°C, 30 cycles of 30 s at 94°C, 30 s at 60°C, and 1 min at 72°C and a final extension for 10 min at 72°C. PCR products were separated by agarose gel electrophoresis (1%) in Tris-acetate/EDTA buffer and visualized using GelRed (Biotium, Hayward, CA). Both primer sets CfdJ_NH_F/CfdJ_NH_R and CfdJ_NN_F/CfdJ_NH_R target the 2266 bp region of the *cfdJ* gene, excluding the 87 bp 5′ sequence encoding a predicted 29 amino acid cleavable signal peptide for secretion. The amplicons CfdJ_NH and CfdJ_NN were digested with either EcoRI and BamHI, or NcoI and BamHI (Thermo Fisher Scientific) respectively. After digestion, the fragments were ligated into plasmid pET28a using T4 DNA ligase (Thermo Fisher Scientific) creating plasmids pCfdJ_NH and pCfdJ_NN. The sequences of the inserts were verified by Sanger sequencing (GATC Biotech) and plasmids were transformed into *E.coli* BL21 (DE3). To produce His-tagged CfdJ protein, a 200-mL culture of *E.coli* BL21 (DE3) carrying pCfdJ_NH was grown to an $O.D_{600}$ of 1 at 37°C and induced with 0.5 mM IPTG for 18 hours at 16°C. Cells were harvested by centrifugation at 6

000 g for 15 minutes and washed three times with 50 mM sodium phosphate buffer at pH 7.3. Pellets were frozen at −20°C for one hour, resuspended in 5 mL of His Binding buffer (Zymo Research, Freiburg, Germany) and sonicated for 10 minutes at 40% power with 30 second on-off cycles in a VibraCell VCX 13 sonicator. The lysates were treated with Benzonase nuclease (Sigma Aldrich), centrifuged at 21 000 g for 15 minutes and filtered through a 0.22 μM filter. The N-terminal His-tagged CfdJ protein was purified from the lysate with the His-Spin Protein Miniprep kit as described by the manufacturer (Zymo Research). The protein was desalted and concentrated on an Amicon Ultra-0.5 mL Centrifugal Filter (EMD Millipore). The concentration of the purified protein was quantified with the Qubit Protein Assay (Invitrogen) while visualisation of the protein was done on a 10% SDS-PAGE gel (Biorad Laboratories) with Lumitein staining (Biotium). To produce the CfdJ protein without a His-tag, cell lysates of *E.coli* BL21 (DE3) carrying pCfdJ_NN were prepared as reported above for *E.coli* BL21 (DE3) carrying pCfdJ_NH and the carbofuran hydrolase activity was compared to this in the lysate containing the His-tagged CfdJ protein. The carbofuran hydrolase activities in both lysates were similar.

Determination of enzyme kinetics

The reaction mixtures for determining CfdJ enzyme kinetics contained 0.1, 0.2, 0.3, 0.4, 0.5, 0.6, 0.7, 0.8 and 0.9 mM carbofuran (Sigma Aldrich, Basel, Switzerland) in 50 mM sodium phosphate buffer and 1% DMSO to enhance the solubility of carbofuran. Each reaction mixture contained 11.76 pmol of the purified CfdJ protein within a total volume of 200 μL. Reaction mixtures were incubated at 37°C and the reaction terminated after 0, 30, 60 and 90 minutes by adding 5 μL of 2 mM $HgCl_2$ which is known to inhibit CehA (Hashimoto *et al.*, 2002). The disappearance of carbofuran and the formation of carbofuran phenol (Dr. Ehrenstorfer GmbH) were determined as described above. The rate of carbofuran degradation by CfdJ was plotted as a function of the substrate concentration and the maximum velocity (Vmax), Michaelis-Menten constant (K_M) and the rate constant (*kcat*) values were calculated with nonlinear regression with the GraphPad Prism 5.01 software (GraphPad). Each reaction was performed in triplicate. In a preliminary experiment, identical rates were obtained with 0.25 mM carbofuran in the absence and presence of 1% DMSO showing the addition of 1% DMSO did not affect degradation rates.

Determination of carbamate substrate specificity

To determine the substrate range of CfdJ, 0.5 mM of either aldicarb (2-methyl-2-(methylthio)propanal *O*-(*N*-methylcarbamoyl)oxime), oxamyl (methyl 2-(dimethylamino)-*N*-[(methylcarbamoyl)oxy]-2-oxoethanimidothioate), propoxur (2-isopropoxyphenyl *N*-methylcarbamate), metolcarb (3-methylphenyl methylcarbamate), fenobucarb ((2-butan-2-ylphenyl) *N*-methylcarbamate), carbaryl, carbofuran, isoprocarb (2-propan-2-ylphenyl) *N*-methylcarbamate) or 4-nitrophenyl acetate (Sigma Aldrich) in 50 mM sodium phosphate buffer were incubated at 37°C with 11.76 pmol CfdJ protein in a volume of 200 μL. The structures of all the carbamate pesticides used can be found in the Supporting Information Figure F2. The reactions were terminated after two hours and the disappearance of the substrate measured by UPLC as described above. Hydrolysis of carbaryl was determined by monitoring the appearance of the hydrolysis product 1-naphthol as described (Hashimoto *et al.*, 2002). Hydrolysis of 4-nitrophenyl acetate was measured by monitoring A_{400} as described (Hashimoto *et al.*, 2002). All assays were performed in triplicate.

Construction of CfdJ variants

To eliminate the possibility that the 5' secretory signal sequence might interfere with protein expression in *E. coli*, the *cehA* gene from *Rhizobium* sp. AC100 was custom synthesized without this sequence (Integrated DNA Technologies) and delivered in plasmid pUCIDT-Kan. The *cehA* gene was amplified with primers CfdJ_NN_F and CfdJ_NH_R as described above for the *cfdJ* gene and digested with NcoI and EcoRI. The gene was cloned into plasmid pET28a but without the His-tag. The resulting recombinant plasmid was designated as pCehA_NN. To produce the CfdJ variants, the PCR amplicons generated with primers CfdJ_NN_F and CfdJ_NH_R from both genes were digested with SphI, SacI and HindIII (Fermentas). The resulting fragments were isolated from a 1.5% agarose gel. Hybrids of these fragments were constructed by ligating each *cfdJ* fragment to the complementary *cehA* fragment (Figure 6A). The hybrid genes were then cloned into pET28a and the sequences of the inserts were verified by Sanger sequencing.

Determining the catalytic activity of the CfdJ variants

All proteins were expressed and cell lysates were obtained as described above except that the cells were lysed in sodium phosphate buffer instead of the His-binding buffer. To test the catalytic activity of CfdJ, CehA and the hybrid proteins, 100 μL of cell lysate (4 μg total protein) was incubated with either 0.5 mM carbofuran, carbaryl or oxamyl in sodium phosphate buffer with 1% DMSO at 27°C for 48 hours. An equal amount of cell lysate of *E. coli* BL21 (DE3) carrying pET28a with no insert, as well as 100 μL of sodium phosphate buffer instead of cell lysate were used to assess background hydrolysis. Degradation of carbofuran, carbaryl and oxamyl was determined as described above. The net amount of carbofuran, carbaryl and oxamyl degraded was calculated by subtracting background hydrolysis from the result of each experiment. All assays were performed in triplicate.

Phylogenetic analysis of CfdJ

To search for proteins with similarity to CfdJ, a PSI-blast analysis against the NCBI non-redundant protein sequences (nr) database was performed (Altschul *et al.*, 1997). Sequences to be analysed further were selected based on the alignment score and query coverage. Seventeen protein sequences with an identity of 36-99% to CfdJ were extracted and aligned with the MUSCLE multiple sequence alignment tool of the Geneious 9 software (www.geneious.com). A phylogenetic tree was calculated with the RaxML maximum likelihood tree calculator (Stamatakis *et al.*, 2008). The CAT heterogeneity model and

the JTT amino-acid replacement matrix were used. For each distinct starting tree, 1000 bootstrap replicates were calculated. The final tree was visualized with FigTree V 4.2. The presence of twin arginine translocase (TAT) and secretory (Sec-type) signal peptides for each sequence was predicted by the PRED-TAT software (Bagos *et al*., 2010). The search for conserved domains was performed against the NCBI Conserved Domain Database (Marchler-Bauer *et al*., 2015).

Acknowledgements

This research was supported by the Inter-University Attraction Pole (IUAP) "μ-manager" of the Belgian Science Policy (BELSPO, P7/25), the Flemish Interuniversity Council (VLIR-UOS) of Belgium (BBTP2007-0012-1087), EU project BIOTREAT (EU grant n° 266039) and by the FNRS under grant 'grand equipment' no. 2877824. We thank D. Grauwels for technical support, B. Horemans for assistance with the UHPLC measurements and P. Albers and J. T'Syen for the critical reading of the manuscript.

References

Akashi, H. (1999) Within- and between-species DNA sequence variation and the 'footprint' of natural selection. *Gene* **238:** 39–51.

Altschul, S.F., Madden, T.L., Schaffer, A.A., Zhang, J., Zhang, Z., Miller, W., and Lipman, D.J. (1997) Gapped BLAST and PSI-BLAST: A new generation of protein database search programs. *Nucleic Acids Res* **25:** 3389–3402.

Bagos, P.G., Nikolaou, E.P., Liakopoulos, T.D., and Tsirigos, K.D. (2010) Combined prediction of tat and sec signal peptides with hidden markov models. *Bioinformatics* **26:** 2811–2817.

Breugelmans, P., Leroy, B., Bers, K., Dejonghe, W., Wattiez, R., De Mot, R., and Springael, D. (2010) Proteomic study of linuron and 3,4-dichloroaniline degradation by *Variovorax* sp. WDL1: Evidence for the involvement of an aniline dioxygenase-related multicomponent protein. *Res Microbiol* **161:** 208–218.

Chaudhry, G.R. and Ali, A.N. (1988) Bacterial metabolism of carbofuran. *Appl Environ Microbiol* **54:** 1414–1419.

Chen, Q., Wang, C.H., Deng, S.K., Wu, Y.D., Li, Y., Yao, L., *et al*. (2014) Novel three-component Rieske non-heme iron oxygenase system catalyzing the N-dealkylation of chloroacetanilide herbicides in *Sphingomonads* DC-6 and DC-2. *Appl Environ Microbiol* **80:** 5078–5085.

Desaint, S., Hartmann, A., Parekh, N.R., and Fournier, J. (2000) Genetic diversity of carbofuran-degrading soil bacteria. *FEMS Microbiol Ecol* **34:** 173–180.

Hashimoto, M., Fukui, M., Hayano, K., and Hayatsu, M. (2002) Nucleotide sequence and genetic structure of a novel carbaryl hydrolase gene (*cehA*) from *Rhizobium* sp strain AC100. *Appl Environ Microbiol* **68:** 1220–1227.

Hashimoto, M., Mizutani, A., Tago, K., Ohnishi-Kameyama, M., Shimojo, T., and Hayatsu, M. (2006) Cloning and nucleotide sequence of carbaryl hydrolase gene (*cahA*) from *arthrobacter* sp. RC100. *J Biosci Bioeng* **101:** 410–414.

Hayatsu, M. and Nagata, T. (1993) Purification and characterization of carbaryl hydrolase from *Blastobacter* sp. strain M501. *Appl Environ Microbiol* **59:** 2121–2125.

IUPAC. 2016. *IUPAC Information page on carbofuran* [Online]. http://sitem.herts.ac.uk/aeru/iupac/Reports/118.htm.

Jukes, T. (1980) Silent nucleotide substitutions and the molecular evolutionary clock. *Science* **210:** 973–978.

Karns, J.S., Mulbry, W.W., Nelson, J.O., and Kearney, P.C. (1986) Metabolism of carbofuran by a pure bacterial culture. *Pest Biochem Physiol* **25:** 211–217.

Karns, J.S. and Tomasek, P.H. (1991) Carbofuran hydrolase - purification and properties. *J Agric Food Chem* **39:** 1004–1008.

Kim, I.S., Ryu, J.Y., Hur, H.G., Gu, M.B., Kim, S.D., and Shim, J.H. (2004) *Sphingomonas* sp. strain SB5 degrades carbofuran to a new metabolite by hydrolysis at the furanyl ring. *J Agric Food Chem* **52:** 2309–2314.

Larsen, M.H., Biermann, K., Tandberg, S., Hsu, T., and Jacobs, W.R. Jr. (2007) Genetic manipulation of *Mycobacterium tuberculosis*. *Curr Protoc Microbiol* **10:**

Liu, J., Ng, T., Rui, Z., Ad, O., and Zhang, W. (2014) Unusual acetylation-dependent reaction cascade in the biosynthesis of the pyrroloindole drug physostigmine. *Angew Chem Int Ed Engl* **53:** 136–139.

Marchler-Bauer, A., Derbyshire, M.K., Gonzales, N.R., Lu, S., Chitsaz, F., Geer, L.Y, *et al.* (2015) CDD: NCBI's conserved domain database. *Nucleic Acids Res* **43:** 20.

Naqvi, T., Cheesman, M.J., Williams, M.R., Campbell, P.M., Ahmed, S., Russell, R.J, *et al.* (2009) Heterologous expression of the methyl carbamate-degrading hydrolase MCD. *J Biotechnol* **144:** 89–95.

Nguyen, T.P.O., De Mot, R., and Springael, D. (2015) Draft genome sequence of the carbofuran-mineralizing *novosphingobium* sp. strain KN65.2. *Genome Announcements* **3:** e00764–e00715.

Nguyen, T.P.O., Helbling, D.E., Bers, K., Fida, T.T., Wattiez, R., Kohler, H.P.E, *et al.* (2014) Genetic and metabolic analysis of the carbofuran catabolic pathway in *Novosphingobium* sp KN65.2. *Appl Microbiol Biotechnol* **98:** 8235–8252.

Noor, S., Changey, F., Oakeshott, J.G., Scott, C., and Martin-Laurent, F. (2014) Ongoing functional evolution of the bacterial atrazine chlorohydrolase AtzA. *Biodegradation* **25:** 21–30.

Noor, S., Taylor, M.C., Russell, R.J., Jermiin, L.S., Jackson, C.J., Oakeshott, J.G., and Scott, C. (2012) Intramolecular epistasis and the evolution of a new enzymatic function. *PLoS One* **7:** e39822.

Northrop, D.B. (1998) On the meaning of Km and V/K in enzyme Kinetics. *J Chem Educ* **75:** 1153.

Parekh, N.R., Hartmann, A., and Fournier, J.C. (1996) PCR detection of the *mcd* gene and evidence of sequence homology between the degradative genes and plasmids from diverse carbofuran-degrading bacteria. *Soil Biol Biochem* **28:** 1797–1804.

Peat, T.S., Newman, J., Balotra, S., Lucent, D., Warden, A.C., and Scott, C. (2015) The structure of the hexameric atrazine chlorohydrolase AtzA. *Acta Crystallogr D Biol Crystallogr* **71:** 710–720.

Rousidou, K., Chanika, E., Georgiadou, D., Soueref, E., Katsarou, D., Kolovos, P, *et al.* (2016) Isolation of oxamyl-degrading bacteria and identification of *cehA* as a novel oxamyl hydrolase gene. *Front Microbiol* **7:**

Seffernick, J.L., de Souza, M.L., Sadowsky, M.J., and Wackett, L.P. (2001) Melamine deaminase and atrazine

chlorohydrolase: 98 percent identical but functionally different. *J. Bacteriol.* **183:** 2405–2410.

Shin, D.H., Kim, D.U., Seong, C.N., Song, H.G., and Ka, J.O. (2012) Genetic and phenotypic diversity of carbofuran-degrading bacteria isolated from agricultural soils. *J Microbiol Biotechnol* **22:** 448–456.

Springael, D. and Top, E.M. (2004) Horizontal gene transfer and microbial adaptation to xenobiotics: New types of mobile genetic elements and lessons from ecological studies. *Trend Microbiol* **12:** 53–58.

Stamatakis, A., Hoover, P., and Rougemont, J. (2008) A rapid bootstrap algorithm for the RAxML web servers. *Syst Biol* **57:** 758–771.

T'Syen, J., Tassoni, R., Hansen, L., Sorensen, S.J., Leroy, B., Sekhar, A, *et al.* (2015) Identification of the amidase BbdA that initiates biodegradation of the groundwater micropollutant 2,6-dichlorobenzamide (BAM) in *Aminobacter* sp. MSH1. *Environ Sci Technol* **49:** 11703–11713.

Tomasek, P.H. and Karns, J.S. (1989) Cloning of a carbofuran hydrolase gene from *achromobacter* sp. strain WM111 and its expression in gram-negative bacteria. *J Bacteriol* **171:** 4038–4044.

Topp, E., Hanson, R.S., Ringelberg, D.B., White, D.C., and Wheatcroft, R. (1993) Isolation and characterization of an N-methylcarbamate insecticide-degrading methylotrophic bacterium. *Appl Environ Microbiol* **59:** 3339–3349.

Yan, Q.X., Hong, Q., Han, P., Dong, X.J., Shen, Y.J., and Li, S.P. (2007) Isolation and characterization of a carbofuran-degrading strain *Novosphingobium* sp. FND-3. *FEMS Microbiol Lett* **271:** 207–213.

Supporting information

Additional Supporting Information may be found in the online version of this article at the publisher's web-site:

Table T1. MS/MS analysis results of the *Novosphingobium* sp KN65.2 protein fraction showing carbofuran hydrolase activity after anion exchange, cation exchange and hydrophobic interaction chromatography of a crude protein extract. The 10 proteins are shown for which corresponding peptides were most recovered together with the Paragon score (Shilov et al., 2007), the % sequence coverage (percentage of matching amino acids from identified peptides having confidence greater than or equal to 95% divided by the total number of amino acids in the sequence) and the number of distinct peptides having at least 95% confidence.

Table T2. Members of the proposed new protein family (as represented in Figure 5). n.r= not reported.

Fig. F1. Multiple alignment of protein members of the CfdJ protein family. Black shading indicates identical amino acids, grey shading indicates similar amino acids and white background indicates unrelated amino acids. Consensus sequences are depicted on the top of each alignment. The positions where CfdJ and CehA differ are highlighted with a red box.

Fig. F2. Molecular structures of the carbamate pesticides used in this study. The structure of the naturally occurring carbamate compound physostigmine is given for comparison.